EFFECT OF Sn INCORPORATION ON STRUCTURAL, PHYSICAL AND ELECTRICAL PROPERTIES OF Ge-Se-Sb-Sn THIN FILMS

J.KANG[a,*], R. K. KOTNALA[b], S. K. TRIPATHI[a]
*a*Center of advanced study in Physics, Department of Physics, Panjab University, Chandigarh, India, 160014
*b*CSIR-National Physical Laboratory, Dr. K. S. Krishnan Road, New Delhi, India, 110012

The present work reports the analysis of physical, structural and electrical properties alongwiththeir compositional dependence for $(Ge_{20}Se_{80})_{90-x}Sb_{10}Sn_x$ (x = 2, 4, 6, 10 at %) chalcogenide glassy system. XRDspectra show the amorphous nature of the prepared samples with the possibility of short-range ordering in the samples. Chemically ordered network model, consistent with $(8-N)$ rule, has been utilizedin estimating various physical parameters which reveals that Ge-Se-Sb-Sn glassy systems are thermally stable glasses. The current transport mechanisms have been investigated as a function of temperature in the temperature range $293\,K - 363\,K$ revealing thatthe dc-conduction occurs through an activated process with single activation energy. Meyer-Neldel rule is found to be obeyed. The present study suggests Ge-Se-Sb-Sn glassy system to be an optimal material for utilization in optical devices.

1. Introduction

The group 16 elements of the periodic table −sulphur (S), selenium (Se) and tellurium (Te) are referred to as chalcogens. The group 16 elements doped with elements of group 13 to 15 of the periodic table forms chalcogenide glasses[1]. Chalcogenide glasses, having an energy gap of 3 eV, show semiconducting behaviour[2]. Semiconductors were presumed earlier to exhibit long-range order. For analyzing band structure in amorphous semiconductors,the chemical bonding environment is given more importance than the periodicity[3]. The molecular bonding in chalcogenide glasses is covalent in nature and the components are kept together with attractive vanderwaals forces. In chalcogenide glasses, the lone pairsenhance the bending of the bond angles and hence reduce the strain energy of the system[4]. Hence the atoms form amorphous structures readily when doped with other elements. Elemental or binary glassy systemsexhibit one or two dimensional chain-like or layered structures and thus possess short-range order over a larger extent. In contrast ternary, quaternary and higher multi-component glassy systems exhibita rigid three-dimensional structure and thus possess short-range order over a shorter extent[5].

Chalcogenide glasses are attracting a rigorous research essentially due to their excellent chemical stability in aggressive environments, transparency in the near and far-infrared region, low optical losses, high refraction coefficient and relatively high ion conductivity [6].The distinctive properties viz. lesser phonon energy, larger and wider bandgap, high values of linear as well as non-linear refractive index, extraordinary transmittance range, etc. of these glasses find them a wide usage in photo-detectors, LED, IR sensors, holography and waveguides[7]. Owing to high refractive index values and high non-linearity ($\sim 10^2$ times of silica), chalcogenides are utilized as an ultrafast switch[8]. Due to high chemical and thermal stability, chalcogenide materials eases fabrication of optical devices. Metallic doping in chalcogenides alters the average coordination number as well as produce structural changes viz. flexible ↔ intermediate ↔ rigid, in

---

* Corresponding author: jasmeenkang.008@gmail.com

the glassy matrix[9]. In chalcogenide glasses, almost all the properties are compositional dependent. Therefore the physical, optical, electrical or structural properties can be altered and controlled depending upon utilization requirement[10].

Amorphous Se has been reported to have vast application in various fields like solar technology, lubricants, pharmaceuticals as well as metal coating[11]. It also shows a remarkable feature of reversible phase transformation (amorphous to crystalline transformation). This feature is very useful for optical memory devices. But pure and unalloyed Se has few shortcomings because of its lesser sensitivity, smaller lifetime, poor thermal stability and higher aging effects. To overcome these drawbacks, pure Seis doped with elements like gallium (Ga), germanium (Ge), tin (Sn), arsenic (As), bismuth (Bi), antimony (Sb), lead (Pb), etc. which gives smaller aging effects, higher crystallization temperature, greater hardness, significantly higher sensitivity and high conductivity[12, 13].

The Ge-Se system is being studied extensively these days. When Ge is added to Se, Ge atoms serve as bond modifiers. Ge-atoms cross-link the Se chain structures, enhancing the average bond strength and hence increasing the glass transition temperature[14]. The mechanical constraints theory of Phillips and Thorpe predicts the critical composition for binary chalcogenide glasses of $IV_x^{th} - VI_{100-x}^{th}$ group, at around x = 20 at % with an average coordination number2.4. For all known Ge-Se systems, $Ge_{20}Se_{80}$ with average coordination number 2.4, is the most critical composition[15]. The addition of Sb in Ge-Se system favours the glass formation and has a remarkable influence on the electrical conductivity of Ge-Se binary chalcogenide glasses. Moreover, Ge-Se-Sb glasses have been selected in the manufacturing of optical devices for the reason of having high transparency in the near and mid-infrared regions as well as for possessing great thermal, chemical and elastic properties[16].

In the present work, Sn has been selected as a chemical modifier in Ge-Se-Sb ternary system which may further broaden the glass forming area and can also produce structural and compositional disorder in the system in respect of the ternary glassy system. $(Ge_{20}Se_{80})_{90-x}Sb_{10}Sn_x$ (x = 2, 4, 6, 10 at %) glassy systemshave been synthesized using melt-quenching technique. The thin films, for the mentioned glassy systems, have been synthesized on glass substrates using the vacuum evaporation technique. The thin films are studiedstructurally by X-ray diffraction. The physical parameters − mean bond energy, average coordination number, glass transitition temperature, average number of constraints, cohesive energy, lone pair electrons, heat of atomization, etc. are deduced using differential empirical approaches and their compositional dependence is also discussed in detail. The current conduction mechanism has also been analyzed as a function of temperature within the temperature range 293 K− 363K of Ge-Se-Sb-Sn thin films.

2. Experimental details

Glassy alloys of $(Ge_{20}Se_{80})_{90-x}Sb_{10}Sn_x$ (x = 2, 4, 6, 10 at %) were prepared using conventional melt-quenching technique. The constituent elements (5N pure) were weighed according to their atomic percentages and vacuum-sealed in quartz ampoules (outer diameter ~ 1 cm, inner diameter ~ 0.8 cm and length ~ 12 cm) in a vacuum of 2×10^{-5}mbar. The vacuum-sealed ampoules were placed inside a furnace and the temperature was raised upto 1100 °C at a constant heating rate of 3−4 °C min^{-1}. The ampoules were wobbled regularly for 24 hours at the maximum temperature for making the melt uniform. The quenching was performed in the ice-cold water to get the ingots that were crushed later in the mortar pestle assembly to get the fine powder of the glassy material.

For the preparation of the thin films, Corning 7059 glass slides were utilized as substrates which were cleaned to wash out any particulate contamination. Cleaning methodology included initial washing with water, further cleaning with acetone or ethanol and lastly rinsing with de-ionized water. Thin films of the glassy alloys were prepared using vacuum evaporation technique [vacuum coating unit HINDHIVAC, MODEL:VS-65D] using the inert gas condensation (IGC) technique in the presence of argon (Ar) as inert gas at room temperature and base pressure of

2×10^{-5} mbar. The thin films were placed inside the deposition chamber for 24 hours before taking measurements for achieving thermodynamic equilibrium. The powdered sample was evaporated by using molybdenum (Mo) boats. The deposition rate was kept slow so that the composition of the films nearly equals the composition of the starting bulk material. X-ray diffraction pattern (XRD) of the prepared thin films were recorded using RigakuMiniflex $-$ 600 X-ray diffractometer operated at 40 kV using CuK_α $-$ wavelength ($\lambda = 1.54056$ Å) at a scanning speed of 0.05 $°s^{-1}$ in the 2θ range from $10° - 80°$. For the electrical measurements, indium (In)electrodes are deposited on thin films (electrode spacing 0.8 mm) by thermal evaporation technique under base pressure of 2×10^{-5} mbar. Planar geometry of Inelectrodes is utilizedbecause it establishesgood and stable ohmic contacts for electrical measurements. The electrical measurements of the samples are studied using the two-probe method under vacuum conditions. These measurements are done by mounting the thin films in anespecially devised metallic sample holder, under a vacuum of2×10^{-3} mbar. The temperature dependence of dark conductivity (σ_d) is determined by fitting a small heater with a metallic base below the thin film in the sample holder. A direct current voltage is applied across the thin film using Keithley Electrometer, Model 6517-A, and current is noted using Pico-ammeter (DPM-111 Model). The variation of the temperature is controlled with a variac and recorded using Copper-Constantan thermocouple with one end attached to the sample and other end attached to the temperature sensor.

3. Results and discussion

3.1. Phase-identification

XRD techniqueis utilized for investigating the structural details of $(Ge_{20}Se_{80})_{90-x}Sb_{10}Sn_x$ (x = 2, 4, 6, 10 at %) chalcogenide glassy system. Fig. 1 showsXRD spectraof as-prepared $(Ge_{20}Se_{80})_{90-x}Sb_{10}Sn_x$ (x = 2, 4, 6, 10 at %) samples. It is clearly observed from Fig. 1 that the diffractograms have no sharp peaks present for as-prepared samples, which verifies the amorphous nature of the prepared samples. The humps in the 2θ range viz $25° - 35°$ and $45° - 55°$indicate the possibility of short-range ordering in the glassy systems.
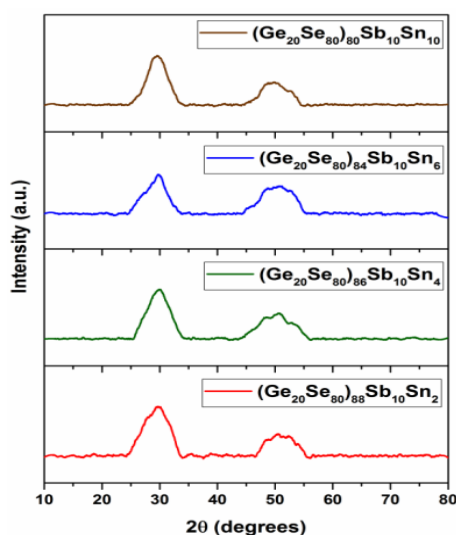

Fig. 1. XRD spectra of $(Ge_{20}Se_{80})_{90-x}Sb_{10}Sn_x$ (x = 2, 4, 6, 10 at %) chalcogenide glasses.

3.2. Physical properties
3.2.1. Number of constraints and average coordination number

The average coordination number ($< r >$) isdescribed as the average atoms coordinated with its nearest neighbour of the constituents. It is quite helpful in understanding the cross-linking. For the composition $(Ge_{20}Se_{80})_{90-x}Sb_{10}Sn_x$ (x = 2, 4, 6 and 10 at %), $< r >$is given by[17]:

$$< r > \ = \ \frac{\alpha Z_{Ge} + \beta Z_{Se} + \gamma Z_{Sb} + \delta Z_{Sn}}{\alpha + \beta + \gamma + \delta} \tag{1}$$

where α, β, γ and δ are the atomicpercentages of Ge, Se, Sb and Sn respectively; Z_{Ge}= 4, Z_{Se} = 2, Z_{Sb} = 3 and Z_{Sn} = 4 represent the coordination numbers (according to 8 − N rule of chemical bond approach with N being the number of valence electrons of respective element) of Ge, Se, Sb and Sn respectively. Thevalues of $< r >$, as determined by Eq. 1, are listed in Table 1. It is observed that $< r >$increases as Sn-content increases. It shows that the cross-linking of chains among the atoms increases as the concentration of Sn increases.

In a glassy system, covalent networks are constrained mechanically by the inter-atomic valence forces namely bond bending and bond stretching. In optimal glass formation, the bond stretching constraints (N_a), the bond bending constraints (N_b) and the average number of constraints (N_c) are given as[18]:

$$N_a \ = \ \frac{< r >}{2} \tag{2}$$

$$N_b = 2< r > - \ 3 \tag{3}$$

$$N_c = \ N_a + \ N_b \tag{4}$$

The calculated values of N_a, N_b and N_c for $(Ge_{20}Se_{80})_{90-x}Sb_{10}Sn_x$(x = 2, 4, 6 and 10 at %) systems are reported in Table 1. The chalcogenide glassy systems can be grouped into three categories viz. (i) over-coordinated or rigid glassy system having $< r >$ greater than 2.4 and N_c greater than 3; (ii) fully coordinated or ideal glassy system having $< r >=$ 2.4 and N_c = 3; (iii) under-coordinated or spongy glassy system having $< r >$ less than 2.4 and N_c less than 3. The values of $< r >$and N_c from Table 1 show that $(Ge_{20}Se_{80})_{90-x}Sb_{10}Sn_x$(x = 2, 4, 6 and 10 at %) glassy systems are rigid or over-coordinated. From literature[17, 18], it is inferred that the rigid systems have higher glass transition temperature and hence appears to be more thermally stable.

3.2.2. Lone pair of electrons and deviation of stoichiometry

In a chalcogenide glassy system, the number of lone-pair electrons (L) is given as[19]:

$$L = V - < r > \tag{5}$$

whereV corresponds to the valence electrons and is given as:

$$V = \ \frac{\alpha w + \beta x + \gamma y + \delta z}{\alpha + \beta + \gamma + \delta} \tag{6}$$

whereα, β, γ and δ are the atomic weight percentages of Ge, Se, Sb and Sn respectively; w = 4, x = 6, y = 5, z = 4 are the number of valence electrons of Ge, Se, Sb and Sn respectively. The presence of enough lone pairs leads to a stable non-crystalline state. The glass-forming ability is highly influenced by the interaction between the lone pair electrons of the crosslinking chalcogen atom and the cations present in the chalcogenide glassy system. The determined values of L and V are mentioned in Table 1. It is observed that the values of L decreases as Sn-concentration increases which is attributed to the enhanced interaction of Sn ions with the bridging Se atoms. The high values of L (L > 1) show that the investigated systems are good glass former[19].

The deviation of stoichiometry (R) is formulated as the ratio of probabilities of covalent bonding of chalcogen atoms to probabilities of covalent bonding of non-chalcogen atoms. For $(Ge_{20}Se_{80})_{90-x}Sb_{10}Sn_x$(x = 2, 4, 6 and 10 at %) glassy systems, R is defined as[19]:

$$R = \frac{\beta Z_{Se}}{\alpha Z_{Ge} + \gamma Z_{Sb} + \delta Z_{Sn}} \qquad (7)$$

whereα, β, γ and δ are the atomic weight percentages of Ge, Se, Sb and Sn respectively; $Z_{Ge} = 4$, $Z_{Se} = 2$, $Z_{Sb} = 3$ and $Z_{Sn} = 4$ represent the coordination numbers of Ge, Se, Sb and Sn respectively. The occurrence of only heteropolar bonds is characterized by the critical value, R = 1. Also the critical value (R =1) determines the least chalcogen concentration for which a chemically ordered glassy network can exist without any metal–metal bond formation. The values of R < 1 is correlated as a chalcogen-poor system whereas the values of R > 1 is correlated as a chalcogen-rich system. The assessed values of R are depicted in Table 1.From Table 1, it is observed that $(Ge_{20}Se_{80})_{90-x}Sb_{10}Sn_x$(x = 2, 4, 6 and 10 at %) glassy systems arechalcogen-rich up to x = 6 at% and becomechalcogen-poor with the further increase in the concentration of Sn to x = 10 at%.
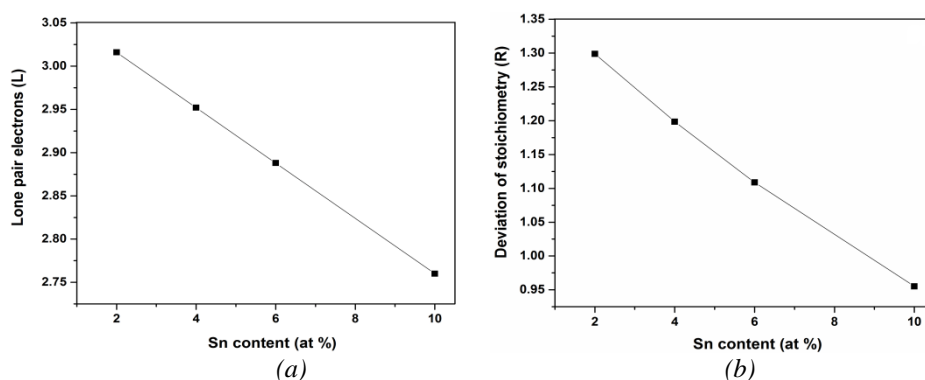

Fig. 2.(a) Plot of lone pair electrons (L) with Sn-content for (Ge$_{20}$Se$_{80}$)$_{90-x}$Sb$_{10}$Sn$_x$ (x = 2, 4, 6 and 10 at%) glassy systems.(b)Compositional dependence of deviation of stoichiometry (R) for (Ge$_{20}$Se$_{80}$)$_{90-}$$_xSb_{10}Sn_x$ (x = 2, 4, 6 and 10 at %) glassy systems.

Table 1.Values of average coordination number (< r >), number of bond stretching constraints (N$_a$), number of bond bending constraints (N$_b$), total number of constraints (N$_c$), valence electrons (V), lone pair electrons (L) and deviation of stoichiometry (R) for (Ge$_{20}$Se$_{80}$)$_{90-x}$Sb$_{10}$Sn$_x$ (x = 2, 4, 6 and 10 at%) glassy systems.

Sample	< r >	N_a	N_b	N_c	V	L	R
$(Ge_{20}Se_{80})_{88}Sb_{10}Sn_2$	2.492	1.246	1.984	3.230	5.508	3.016	1.299
$(Ge_{20}Se_{80})_{86}Sb_{10}Sn_4$	2.524	1.262	2.048	3.310	5.476	2.952	1.199
$(Ge_{20}Se_{80})_{84}Sb_{10}Sn_6$	2.556	1.278	2.112	3.390	5.444	2.888	1.109
$(Ge_{20}Se_{80})_{80}Sb_{10}Sn_{10}$	2.620	1.310	2.240	3.550	5.380	2.760	0.955

3.2.3. Glass transition temperature, mean bond energy and electronegativity

For any glassy system, the values of mean bond energy depend upon certain factors including average coordination number,different types of (homopolar or heteropolar) bonds, the degree of cross-linking per atom, etc. Mean bond energy is represented by< E >and is calculated using the relation described by Ticha et al[20, 21]:

$$< E > = E_{cl} + E_{rm} \qquad (8)$$

whereE_{cl} is the contribution emerging from strong heteropolar bonds and $E_{rm}$is contribution emerging from weaker bonds that form once the strong bonds are maximized. The average energy of cross-linking is calculated as:

$$E_{cl} = P_p E_{hb} \qquad \text{for R} < 1 \tag{8a}$$

$$E_{cl} = P_r E_{hb} \qquad \text{for R} > 1 \tag{8b}$$

whereE_{hb} is the average heteropolar bond energy for glasses with composition $Ge_\alpha Se_\beta Sb_\gamma Sn_\delta$. It is calculated using the relation:

$$E_{hb} = \frac{\alpha Z_{Ge} E_{Ge-Se} + \gamma Z_{Sb} E_{Sb-Se} + \delta Z_{Sn} E_{Sn-Se}}{\alpha Z_{Ge} + \gamma Z_{Sb} + \delta Z_{Sn}} \tag{8c}$$

whereE_{Ge-Se}, E_{Sb-Se} and E_{Sn-Se} are the heteropolar bond energies for Ge−Se, Sb−Se and Sn−Se respectively. The degrees of cross-linking P_p (for R < 1) and P_r (for R > 1) are given by:

$$P_p = \frac{\beta Z_{Se}}{\alpha + \beta + \gamma + \delta} \tag{8d}$$

$$P_r = \frac{\alpha Z_{Ge} + \gamma Z_{Sb} + \delta Z_{Sn}}{\alpha + \beta + \gamma + \delta} \tag{8e}$$

The average energy of the remaining matrix is calculated as:

$$E_{rm} = \frac{2(0.5 < r > - P_r)E_{Se-Se}}{< r >} \qquad \text{for R} > 1 \tag{8f}$$

$$E_{rm} = \frac{2(0.5 < r > - P_p)E_{<>}}{< r >} \qquad \text{for R} < 1 \tag{8g}$$

where$E_{<>} = \frac{1}{6}(E_{Ge-Ge} + E_{Sb-Sb} + E_{Sn-Sn} + E_{Ge-Sb} + E_{Sn-Sb} + E_{Sn-Ge})$ \tag{8h}

Hence in $Ge_\alpha Se_\beta Sb_\gamma Sn_\delta$ glassy system, for selenium-rich region (R > 1), we evaluate as:

$$E_{cl} = \alpha Z_{Ge} E_{Ge-Se} + \gamma Z_{Sb} E_{Sb-Se} + \delta Z_{Sn} E_{Sn-Se} = 4\alpha E_{Ge-Se} + 3\gamma E_{Sb-Se} + 4\delta E_{Sn-Se} \tag{9a}$$

$$E_{rm} = \frac{(\beta Z_{Se} - \alpha Z_{Ge} - \gamma Z_{Sb} - \delta Z_{Sn})E_{Se-Se}}{< r >} = \frac{(2\beta - 4\alpha - 3\gamma - 4\delta)E_{Se-Se}}{< r >} \tag{9b}$$

and for selenium-poor region (R < 1), we evaluate as:

$$E_{cl} = \frac{\beta Z_{Se}(\alpha Z_{Ge} E_{Ge-Se} + \gamma Z_{Sb} E_{Sb-Se} + \delta Z_{Sn} E_{Sn-Se}}{\alpha Z_{Ge} + \gamma Z_{Sb} + \delta Z_{Sn}} = \frac{2\beta(4\alpha E_{Ge-Se} + 3\gamma E_{Sb-Se} + 4\delta E_{Sn-Se}}{4\alpha + 3\gamma + 4\delta} \tag{10a}$$

$$E_{rm} = \frac{(\alpha Z_{Ge} + \gamma Z_{Sb} + \delta Z_{Sn} - \beta Z_{Se})E_{<>}}{<r>} = \frac{(4\alpha + 3\gamma + 4\delta - 2\beta)E_{<>}}{<r>} \tag{10b}$$

The bond energy of heteropolar bonds are calculated by the method suggested by Pauling[22]:

$$E_{A-B} = (E_{A-A} \times E_{B-B})^{1/2} + 30(\chi_A - \chi_B)^2 \tag{11}$$

whereE_{A-B} is the bond energy of heteropolar bond, E_{A-A} and E_{B-B} are the bond energies of homopolar bonds. The bond energies of the homopolar bonds are taken as E_{Ge-Ge} = 37.60 kcal/mol, E_{Se-Se} = 44.00 kcal/mol, E_{Sb-Sb} = 30.20 kcal/mol and E_{Sn-Sn} = 34.20 kcal/mol respectively. χ_{Ge} = 2.01, χ_{Se} = 2.55, χ_{Sb} = 2.05 and χ_{Sn} = 1.96 are the electronegativity values of Ge, Se, Sb and Sn respectively. Table 2 lists the evaluated heteropolar bond energies.

Table 2. Bond energies of heteropolar bonds for $(Ge_{20}Se_{80})_{90-x}Sb_{10}Sn_x$ (x = 2, 4, 6 and 10 at %) glasses.

Bond	Bond energy (kcal/mol)
Ge−Se	49.42
Sb−Se	43.95
Sn−Se	49.23

Using Eq. 8, 9 and 10,the values of $<E>$for $(Ge_{20}Se_{80})_{90-x}Sb_{10}Sn_x$ (x = 2, 4, 6 and 10 at %) glassy systems have been estimated and are depicted in Table 3. It is observed that $<E>$ increases as Sn-content increases. The increased values of $<E>$are due to the higher bond energies of Sn−Se bonds as compared to the weaker Se−Se bonds. The calculated values of $<E>$are utilized in assessing the glass transition temperature (T_g) using the empirical relation proposed by Tichy-Ticha[20, 21]:

$$T_g = 311(<E> - 0.9) \tag{12}$$

Table 3 lists the calculated values of T_g using Eq. 12. T_g values are observed to increase with the increasing Sn-concentration. The increased values of $T_g$owes to the increase in density of samples with Sn-content along with the cause for the increase in $<E>$. The higher glass transition temperatures suggest that $(Ge_{20}Se_{80})_{90-x}Sb_{10}Sn_x$(x = 2, 4, 6 and 10 at %) are thermally stable glasses.

The electronegativity (χ) has been calculated using Sanderson's principle[23]. According to this principle, χ of the glassy system is determined by taking geometric mean of the electronegativity of its constituent elements. For $(Ge_{20}Se_{80})_{90-x}Sb_{10}Sn_x$ (x = 2, 4, 6 and 10 at %) glassy systems, χ is given as:

$$\chi = \left[(\chi_{Ge})^a(\chi_{Se})^b(\chi_{Sb})^c(\chi_{Sn})^d\right] \tag{13}$$

where a, b, c and d are the atomic fractions of Ge, Se, Sb and Sn respectively. $\chi_{Ge} = 2.01$, $\chi_{Se} = 2.55$, $\chi_{Sb} = 2.05$ and $\chi_{Sn} = 1.96$ are the electronegativity values of Ge, Se, Sb and Sn respectively. The evaluated values of χ for Ge-Se-Sb-Sn glassy system is mentioned in Table 4. χ of the glassy system decreases with the increase in Sn-content.

3.2.4. Theoretical bandgap and average heat of atomization

The heat of atomization is defined as the energy required to dissociate one mole of a substance into isolated atoms. The average heat of atomization characterizes cohesive energy and hence determines the relative bond strength between the isostructural materials. The values of average heat of atomization $<H_s>$for Ge-Se-Sb-Sn glasses are estimated by using the relation[24]:

$$<H_S> = \frac{\alpha H_s^{Ge} + \beta H_s^{Se} + \gamma H_s^{Sb} + \delta H_s^{Sn}}{\alpha + \beta + \gamma + \delta} \tag{14}$$

whereα, β, γ and δ are the atomic weight percentages of Ge, Se, Sb and Sn respectively; $H_s^{Ge} = 377$ kJ/mol,$H_s^{Se} = 227$ kJ/mol, $H_s^{Sb} = 262$ kJ/mol and $H_s^{Sn} = 302$ kJ/mol are the values of heat of atomization of Ge, Se, Sb and Sn respectively. The evaluated values of $<H_s>$ are depicted in Table 3. It has been seen that the values of$<H_s>$ increases with the incorporation of Sn which supports the enhanced rigidity of the present Ge-Se-Sb-Sn glassy systems.

The values of the theoretical bandgap (E_g^{th}) for the present glassy alloys areevaluated by using the empirical relation[25]:

$$E_g^{th} = v_{Ge}E_g(Ge) + v_{Se}E_g(Se) + v_{Sb}E_g(Sb) + v_{Sn}E_g(Sn) \tag{15}$$

where v_{Ge}, v_{Se}, v_{Sb} and v_{Sn} are the volume fractions of Ge (13.63 cm³/mol), Se(16.42 cm³/mol), Sb (18.19 cm³/mol) and Sn (16.24 cm³/mol) respectively; $E_g(Ge) = 0.67$ eV, $E_g(Se) = 1.95$ eV, $E_g(Sb) = 0.101$ eV and $E_g(Sn) = 0.08$ eV are the energy gaps of Ge, Se, Sb and Sn respectively. The assessed values of E_g^{th} are depicted in Table 3 and are observed to decrease as Sn-content is increased. These results are supported by the decrease in average single bond energy defined by the ratio of $<H_s>$ to$<r>$[26]. The values of average single bond energy are also found to decrease with the incorporation of Sn. The absorption edge (λ)is estimated from E_g^{th}. The values ofλ are recorded in Table 3, suggesting that the optical transmission will be above 900nm. This makes Ge-Se-Sb-Sn glassy systems optimal material for new generation infrared optical systems.
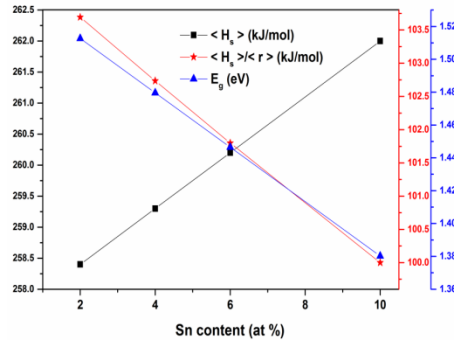

Fig. 3. Compositional variation of average heat of atomization ($<H_s>$), single bond energy ($<H_s>/<r>$), and theoretical bandgap (E_g^{th}) for $(Ge_{20}Se_{80})_{90-x}Sb_{10}Sn_x$ (x = 2, 4, 6 and 10 at %) glassy systems.

Table 3. Values of mean bond energy ($<E>$), glass transition temperature (T_g), average heat of atomization ($<H_s>$), average single bond energy ($<H_s>/<r>$), theoretical band gap (E_g^{th}) and absorption edge (λ) for $(Ge_{20}Se_{80})_{90-x}Sb_{10}Sn_x$ (x = 2, 4, 6 and 10 at %) glassy systems.

Sample	$<E>$per atom (eV)	T_g (K)	$<H_s>$ (kJ/mol)	$<H_s>/<r>$ (kJ/mol)	E_g^{th} (eV)	λ (nm)
$(Ge_{20}Se_{80})_{88}Sb_{10}Sn_2$	2.50	497.45	258.40	103.69	1.51	817
$(Ge_{20}Se_{80})_{86}Sb_{10}Sn_4$	2.56	516.35	259.30	102.73	1.48	835
$(Ge_{20}Se_{80})_{84}Sb_{10}Sn_6$	2.62	535.85	260.20	101.80	1.45	854
$(Ge_{20}Se_{80})_{80}Sb_{10}Sn_{10}$	2.71	561.66	262.00	100.00	1.38	895

3.2.5. Density, molar volume, packing density and compactness

Density (ρ) measures the rigidity of the system. For Ge-Se-Sb-Sn glassy systems, ρ has been determined using the formulae[27]:

$$\rho = \left(\Sigma \frac{m_i}{d_i}\right)^{-1} = \left(\frac{m_{Ge}}{d_{Ge}} + \frac{m_{Se}}{d_{Se}} + \frac{m_{Sb}}{d_{Sb}} + \frac{m_{Sn}}{d_{Sn}}\right)^{-1} \quad (16)$$

where m_{Ge}, m_{Se}, m_{Sb} and m_{Sn} are the mass fractions of Ge (72.64 amu), Se (78.96 amu), Sb (121.76 amu) and Sn (118.71amu) respectively whereasthe values of d_{Ge}, d_{Se}, d_{Sb} and d_{Sn} are taken as 5.323 gcm⁻³, 4.819 gcm⁻³, 6.684 gcm⁻³ and 7.31 gcm⁻³ respectively.

Molar volume (V_m) has been evaluated using the value of density expression[27]:

$$V_m = \frac{\Sigma x_i M_i}{\rho} = \frac{aM_{Ge} + bM_{Se} + cM_{Sb} + dM_{Sn}}{\rho} \quad (17)$$

where a, b, c and d are the atomic fractions and M_{Ge}, M_{Se}, M_{Sb} and M_{Sn} are the molar masses of Ge, Se, Sb and Sn respectively.

Packing density is formulated as the ratio of used space to the allocated space and is calculated using the relation[27]:

$$\text{Packing density} = \frac{N \times \rho}{M} \tag{18}$$

where N is the Avogadro's number, ρ is the calculated density and M is the molecular weight of the respective composition of $(Ge_{20}Se_{80})_{90-x}Sb_{10}Sn_x$ (x = 2, 4, 6 and 10 at %) glassy systems.

Compactness is formulated as the measure of normalized change of mean atomic volume caused by the chemical interaction of elements forming the glassy network. Compactness is more sensitive to changes in the structure of the glass network as compared to the mean atomic volume. The compactness of structure isdetermined according to formulae[27]:

$$\text{Compactness} = \frac{\Sigma \frac{x_i M_i}{\rho_i} - \Sigma \frac{x_i M_i}{\rho}}{\Sigma \frac{x_i M_i}{\rho}} \tag{19}$$

where x_i, M_i, and ρ_i are atomic fraction, atomic weight and atomic density of ith element of glassy system. The evaluated values of ρ, V_m, packing density and compactness from Eq. 16, 17, 18 and 19 respectively are depicted in Table 4. It is inferred that ρ and V_m values for Ge-Se-Sb-Sn glasses increases with the increase in Sn content. The density (5.323 gcm^{-3}) and mass (72.64 amu) of Ge as well as the density (4.819 gcm^{-3}) and mass (78.96 amu) of Se are very low as compared to heavier Sn with density (7.310 gcm^{-3}) and mass (118.71 amu). So as the concentration of Sn is increased, Ge and Se atoms are replaced by heavier and denser Sn, which leads to the increase in ρ and V_m. Further, the addition of Sn content enhances the cross-linking in the glassy network and hence rigidity increases due to which ρ increases also. Fig. 4 shows the variation of ρ and V_m with $< r >$.
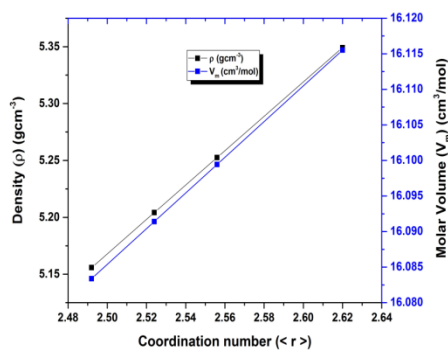

Fig. 4. Variation of density (ρ) and molar volume (V_m) for $(Ge_{20}Se_{80})_{90-x}Sb_{10}Sn_x$ (x = 2, 4, 6 and 10 at %) glasses as a function of average coordination number ($< r >$).

The calculated values of compactness show a decrease in the value with the incorporation of Sn (up to x = 4 at%) and an increase with the further addition of Sn (x = 6 and 10 at%). Thus one can expect that the micro-hardness of the samples increases with the increase in its compactness. The negative values of compactness correspond to higher free volumes and flexibilities. The average coordination number dependence of the compactness for Ge-Se-Sb-Sn glassy systems is shown in Fig. 5. From Fig. 5, it is evident that the minima of the compactness occur at $< r >$ = 2.524 for the investigated glassy system. This shows that the system has the highest mean atomic volume of the network for x = 4 at % composition of $(Ge_{20}Se_{80})_{90-x}Sb_{10}Sn_x$ glassy system.
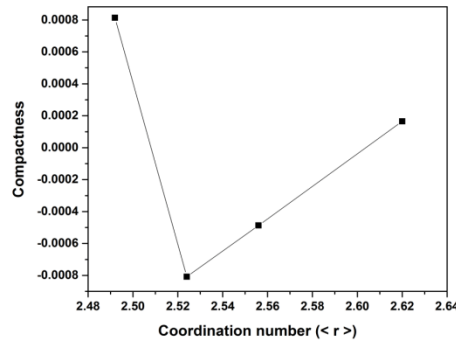
Fig. 5. Variation of compactness with the average coordination number ($< r >$) for $(Ge_{20}Se_{80})_{90-x}Sb_{10}Sn_x$ ($x = 2, 4, 6$ and 10 at %) glassy systems showing that the minima of the compactness occur at $x = 4$ at %.

Table 4. Values of electronegativity (χ), density (ρ), molar volume (V_m), packing density and compactness for $(Ge_{20}Se_{80})_{90-x}Sb_{10}Sn_x$ ($x = 2, 4, 6$ and 10 at%) glassy systems.

Sample	χ	ρ (gcm^{-3})	V_m (cm^3/mol)	Packing density (10^{22} atoms/cm^3)	Compactness
$(Ge_{20}Se_{80})_{88}Sb_{10}Sn_2$	2.38	5.16	16.08	3.744	0.00081
$(Ge_{20}Se_{80})_{86}Sb_{10}Sn_4$	2.37	5.20	16.09	3.742	-0.00080
$(Ge_{20}Se_{80})_{84}Sb_{10}Sn_6$	2.36	5.25	16.10	3.740	-0.00049
$(Ge_{20}Se_{80})_{80}Sb_{10}Sn_{10}$	2.34	5.35	16.11	3.737	0.00016

3.2.6. Distribution of bonds and cohesive energy

The cohesive energy (CE) of any system is specified as the energy required in the stabilization of an infinitely large collection of materials per atom which allows the determination of the number of probable bonds. It helps in determining the magnitude of the bond strength. In general, it is found that Zachariasen assumption [28]is obeyed in a glass structure which suggests that the probability of bond-formation among dissimilar atoms is higher than the probability of bond-formation among similar atoms. Therefore, according to this assumption, bonds between similar atoms will form only when there is an excess of similar atoms. Also the bond-formation occur in the decreasing order of bond energies until all the existing valences for the atoms are saturated. So according to this model, the bond energies are assumed to be additive. Thus CE is evaluated by adding the bond energies of the overall bond expected in the alloy[27]:

$$CE = \Sigma C_i D_i \tag{20}$$

where C_i is the number of expected chemical bond and D_i is the corresponding bond energy of the occurring bond in the glassy system. The distribution of bonds and CEfor $(Ge_{20}Se_{80})_{90-x}Sb_{10}Sn_x$($x = 2, 4, 6$ and 10 at %) chalcogenides are depicted in Table 5. From the data, it is very evident that CE increases with the incorporation of Sn at the cost of Ge and Se up to $x = 6$ at% due to the formation of strongerheteropolarSn$-$Se bonds. With further incorporation of Sn (up to $x = 10$ at%), the formation of Sb$-$Sb bonds lower down CE. The large and increased values of CE confirm that $(Ge_{20}Se_{80})_{90-x}Sb_{10}Sn_x$ glasses are highly stable glasses making them optimal materials for utilization in optoelectronic devices.

Table 5.Distribution of chemical bonds and cohesive energy (CE) for $(Ge_{20}Se_{80})_{90-x}Sb_{10}Sn_x$
(x = 2, 4, 6 and 10 at%) glassy systems.

Sample	Distribution of chemical bonds					CE (kcal/mol)
	Ge−Se	Sn−Se	Sb−Se	Se−Se	Sb−Sb	
$(Ge_{20}Se_{80})_{88}Sb_{10}Sn_2$	0.59935	0.06813	0.19333	0.13919	−	47.60
$(Ge_{20}Se_{80})_{86}Sb_{10}Sn_4$	0.57806	0.13447	0.19080	0.09666	−	47.83
$(Ge_{20}Se_{80})_{84}Sb_{10}Sn_6$	0.55732	0.19911	0.18833	0.05524	−	48.05
$(Ge_{20}Se_{80})_{80}Sb_{10}Sn_{10}$	0.42677	0.26681	0.15143	−	0.15499	45.56

3.3. Electrical properties

Fig. 6 depicts the current-voltage plots on a log-log scale for $(Ge_{20}Se_{80})_{90-x}Sb_{10}Sn_x$ (x = 2, 4, 6 and 10 at%) thin films. The plots are linear with slope almost unity upto the operating range of applied voltage (0 V−100 V) and hence indicating the ohmicbehaviour of the contacts.
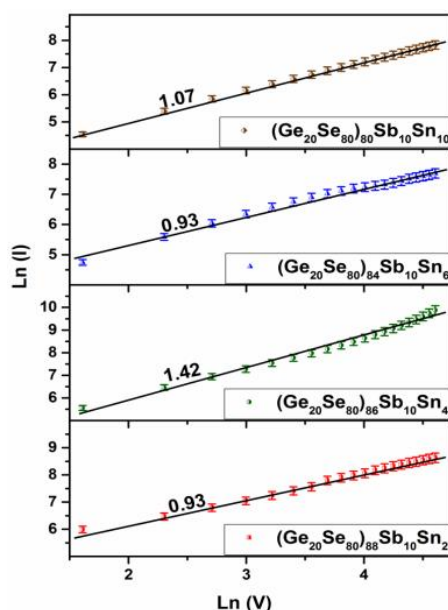

Fig. 6. The plots of ln (I) against ln (V) for $(Ge_{20}Se_{80})_{90-x}Sb_{10}Sn_x$ (x = 2, 4, 6 and 10 at %) thin films indicating the ohmicbehaviour of the contacts.

The dcconductivity measurements in chalcogenide glasses provides valuable knowledge about the transport mechanism. To investigate the current transport behaviour temperature-dependent σ_d measurements are performed in the temperature range 293 K− 363 K for Ge-Se-Sb-Sn thin films which shows typical Arrhenius type of activation[29]:

$$\sigma_d T^{1/2} = \sigma_o \exp\left(-\frac{E_a}{k_B T}\right) \qquad (21)$$

whereσ_o is the pre-exponential factor, E_a is the conduction activation energy, T is the absolute temperature and k_B is the Boltzmann constant.The values of E_a and $\sigma_o$are calculated from the slope and intercept of ln $(\sigma_d T^{1/2})$ against T^{-1} plot. Fig. 7 depicts the variation of ln $(\sigma_d T^{1/2})$ against

T^{-1} for Ge-Se-Sb-Sn thin films within the temperature range 293 K− 363K. The straight line behaviour of the plots depicted in Fig. 7 in the studied temperature range suggests that the conduction in the glassy systemsoccurs via an activated process exhibitingsingle activation energy in this particular temperature range.
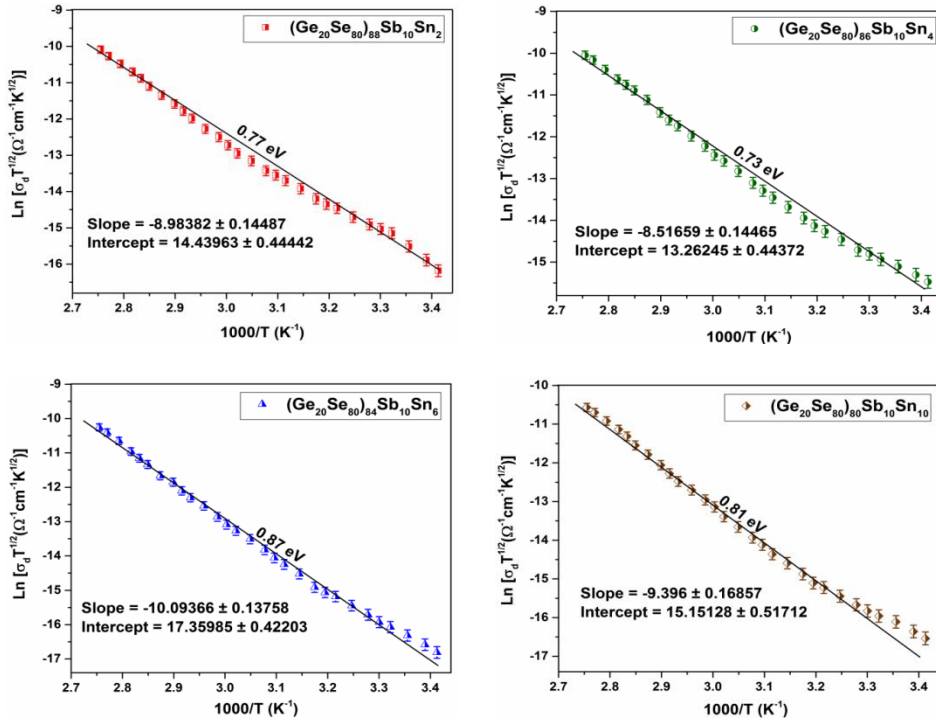

Fig. 7. Plots of ln $(\sigma_d T^{1/2})$ against T^{-1} in the temperature range (293 K − 363 K) for $(Ge_{20}Se_{80})_{90-x}Sb_{10}Sn_x$ (x = 2, 4, 6 and 10 at %) thin films depicting the values of activation energies also.

As the activation energies and temperature range are too high to observe hopping so thermally assisted tunneling has been investigated, which is given as[29]:

$$\sigma_d = \sigma_o \left(1 + \frac{F^2}{6}T^2\right) \tag{22}$$

where σ_o and F are constants.Fig. 8(a) represents the variation of σ_d versus T^2 for Ge-Se-Sb-Sn thin films. The non-linear plots clearly indicate that the tunneling mechanism is not the dominant conduction mechanism in Ge-Se-Sb-Sn thin films in this temperature range. Therefore the conduction mechanism predominating the mentioned temperature range is thermionic emission only. It is factual that thermally activated phenomena like dc-conduction in chalcogenide glasses obeys Meyer-Neldel (MN) rule which is given as[30]:

$$\sigma_o = \sigma_{oo} \exp\left(\frac{E_a}{E_{MN}}\right) \tag{23}$$

where σ_{oo} is MN pre-exponent factor and E_{MN} is MN characteristic energy. Fig. 8(b) depicts the plot of ln (σ_o) against E_a for Ge-Se-Sb-Sn thin films. The linear plot infers that σ_o varies exponentially with E_a according to Eq. 23 and hence MN rule is obeyed in all compositions of Ge-Se-Sb-Sn thin films. The slope and intercept of the straight-line plot in Fig. 8(b) yields MN characteristic energy (E_{MN} = 33.64 meV) and MN pre-exponential factor (σ_{oo} = 1.779 × $10^{-4}\Omega^{-1}cm^{-1}$). The values are close to the range suggested by Shimakawa and Abdel-Wahab for chalcogenide glasses[30].

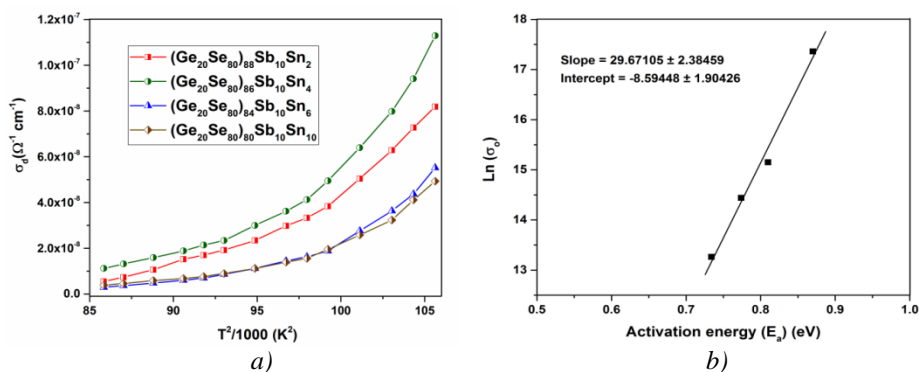Fig. 8. (a) Plots of σ_d against T^2 for $(Ge_{20}Se_{80})_{90-x}Sb_{10}Sn_x$ (x = 2, 4, 6 and 10 at %) thin films in the temperature range (293 K − 363 K). (b) Validation of Meyer-Neldel rule in $(Ge_{20}Se_{80})_{90-x}Sb_{10}Sn_x$ (x = 2, 4, 6 and 10 at %) thin films.

Table 6. Values of conductivity (σ_d) at 298 K, activation energy (E_a) and pre-exponent factor (σ_o) for all compositions of $(Ge_{20}Se_{80})_{90-x}Sb_{10}Sn_x$ (x = 2, 4, 6 and 10 at %) thin films.

Sample	σ_d ($\Omega^{-1}cm^{-1}$) at 298 K	E_a (eV)	σ_o ($\Omega^{-1}cm^{-1}$)
$(Ge_{20}Se_{80})_{88}Sb_{10}Sn_2$	1.06×10^{-8}	0.77	1.87×10^6
$(Ge_{20}Se_{80})_{86}Sb_{10}Sn_4$	1.59×10^{-8}	0.73	5.75×10^5
$(Ge_{20}Se_{80})_{84}Sb_{10}Sn_6$	4.75×10^{-9}	0.87	3.46×10^7
$(Ge_{20}Se_{80})_{80}Sb_{10}Sn_{10}$	5.84×10^{-9}	0.81	3.80×10^6

Table 6 represents the values of σ_d at 293 K, E_a and σ_o for Ge-Se-Sb-Sn thin films. It is observed that σ_o is not constant for the series under investigation. Further the values of σ_o increases as the value of E_a increases. Moreover, the variation in the values of σ_d as well as E_a is very low with the incorporation of Sn. σ_d values increase as Sn-concentration is increased to x = 4 at%. With the further addition of Sn (to x = 6 at% and 10 at%) σ_d values decrease.

The results are interpreted with reference to the structural changes taking place after the addition of Sn. The incorporation of Sn leads to the substitution of Ge-atoms and the formation of Sn−Se bonds. The Sn−Se iono-covalent bonds (as Sn is more electropositive than Ge), in contrast to Ge−Se bonds, offer more conducting path in the system and hence σ_d increases as Sn concentration increases to x = 4 at%. This rise in σ_d is responsible for the decrease in E_a. With the further increament in Sn content (to x = 6 at% and 10 at %) weaker Sb−Sb bonds formation occurs that leads to more disordering in the system and thereby decreasing σ_d (hence E_a also increases). From Table 6, it is very evident that $(Ge_{20}Se_{80})_{86}Sb_{10}Sn_4$ is the most conducting as compared to others in the series.

4. Conclusions

In the present work, the effect of the addition of Sn on the structural, physical and electrical properties of vacuum evaporated $(Ge_{20}Se_{80})_{90-x}Sb_{10}Sn_x$ (x = 2, 4, 6 and 10 at %) thin films has been studied. The samples have been found amorphous in nature by XRD technique with the possibility of short-range ordering in the glassy systems. The temperature-dependent dark conductivity measurements in the temperature range 293 K−363 K affirms that the conduction in

Ge-Se-Sb-Sn thin films is through an activated process with single activation energy and $(Ge_{20}Se_{80})_{86}Sb_{10}Sn_4$ composition has the highest conductivity as compared to the other compositions in the series. The formation of weaker $Sb-Sb$ bonds leads to a decrease in conductivity for the higher concentration of Sn element. Meyer-Neldel rule is obeyed by $(Ge_{20}Se_{80})_{90-x}Sb_{10}Sn_x$ (x = 2, 4, 6 and 10 at %) glassy systems.

The number of constraints and average coordination number values confirm Ge-Se-Sb-Sn glassy systems to be rigid and over-coordinated. The prepared $(Ge_{20}Se_{80})_{90-x}Sb_{10}Sn_x$ (x = 2, 4 and 10 at %) chalcogenidesare selenium-rich up to x = 6 at% and turns to selenium-poor for x = 10 at%. The high lone pair electrons suggest that Ge-Se-Sb-Sn systems are good glass former. The highglass transition temperaturesconfirm Ge-Se-Sb-Sn glasses to be thermally stable The deep analysis of the physical, electrical and structural properties and the variation of these properties as a function of Sn-content suggest the utilization of these glasses in optical devices (in the near and mid-IR region).

Acknowledgments

References

[1] P. Sharma, N. Sharma, S. Sharda, S.C. Katyal, V. Sharma, Progress in Solid State Chemistry **44**(4), 131 (2016).
[2] V. Sharma, S. Sharda, N. Sharma, S.C. Katyal, P. Sharma, Progress in Solid State Chemistry **54**, 31 (2019).
[3] A.V. Kolobov, P. Fons, J. Tominaga, Physical Review B **87**(15),155204 (2013).
[4] P. Sharma, Applied Physics A, **122**, 402 (2016).
[5] I. Pethes, R. Chahal, V. Nazabal, C. Prestipino, A. Trapananti, S. Michalik, P. Jovari, TheJournal of Physical Chemistry B **120**(34), 9204 (2016).
[6] P. Kumar, J. Kaur, S.K. Tripathi, I. Sharma, Indian Journal of Physics **91**, 1503 (2017).
[7] A.S. Hassanien, I. Sharma, A.A. Akl, Journal of Non-Crystalline Solids **531**, 119853 (2020).
[8] J.K. Behera, X. Zhou, J. Tominaga, R.E. Simpson, Optical Material Express **7**(10), 3741 (2017).
[9] A.S. Hassanien, A.A. Akl, Journal of Non-Crystalline Solids **428**, 112 (2015).
[10] I. Sharma, P. Kumar, S.K. Tripathi, Phase Transitions **90**(7), 653 (2017).
[11] H.E. Atyia, A.S. Farid, Journal of Crystal Growth **436**, 125 (2016).
[12] R. Svoboda, M. Kincl, J. Malek, Journal of Alloys and Compounds **644**, 40 (2015).
[13] S.K. Tripathi, S. Gupta, F.I. Mustafa, N. Goyal, G.S.S. Saini, Journal of Physics D: Applied Physics, **42**,185404 (2009).
[14] R. Golovchak, A. Kozdras, T. Hodge, J. Szlezak, C. Boussard-Pledel, Y. Shpotyuk, B. Bureau, Journal of Alloys and Compounds **750**, 721 (2018).
[15] J.C. Phillips, M.F. Thorpe, Solid State Communications **53**(8), 699 (1985).
[16] I. Sharma, S.K. Tripathi, P.B. Barman, Phase Transitions **87**(4), 363 (2014).
[17] E. Sharma, H.H. Hegazy, V. Sharma, P. Sharma, Physica B: Condensed Matter **562**, 100 (2019).
[18] G.A.M. Amin, A.F. Maged, Materials Chemistry and Physics **97**(2-3), 420 (2006).
[19] P. Vashist, Anjali, B.S. Patial, N. Thakur, AIP Conference Proceedings **1953**(1), 090085(2018).
[20] L. Tichy, H. Ticha, Journal of Non-Crystalline Solids **189**(1-2), 141 (1995).
[21] L. Tichy, H. Ticha, Materials Letters **21**(3-4), 313 (1994).
[22] L. Pauling, Journal of the American Chemical Society**53**(4), 1367 (1931).
[23] R.T. Sanderson, Journal of Chemical Education **65**(2), 112 (1988).
[24] V. Sadagopan, H.C. Gatos, Solid-State Electronics **8**(6), 529 (1965).

[25] P. Kumar, S.K. Tripathi, I. Sharma, Journal of Alloys and Compounds **755**, 108 (2018).
[26] S.S. Fouad, M.S. El-Bana, P. Sharma, V. Sharma, Applied Physics A **120**, 137 (2015).
[27] S. Sharda, N. Sharma, P. Sharma, V. Sharma, Chalcogenide Letters **9**(9),389 (2012).
[28] W.H. Zachariasen, Journal of the American Chemical Society **54**(10), 3841 (1932).
[29] B. Singh, J. Singh, J. Kaur, R.K. Moudgil, S.K. Tripathi, Journal of Materials Science: Materials in Electronics **27**, 8701 (2016).
[30] K. Shimakawa, F. Abdel-Wahab, Applied Physics Letters **70**(5), 652 (1997).